Smart soiling sensor for PV modules

Smart Soiling Sensor for PV Modules

M. Simonazzi, G. Chiorboli, P. Cova, R. Menozzi, D. Santoro,
S. Sapienza, C. Sciancalepore, G. Sozzi, N. Delmonte

Department of Engineering and Architecture, University of Parma
Parco Area delle Scienze 181A, 43124 Parma, Italy

Abstract – In this work we propose a new sensor concept to evaluate the degradation of PV arrays due to soiling. It is based on I-V curve analysis coupled with artificial vision inspection of a reference PV module to quantify and identify the type of dirt. In order to assess the usefulness of this approach in the automatic scheduling of maintenance interventions in smart-grid PV modules, we developed a Simulink model of a DC nanogrid to test different control strategies. Early experimental results are also shown demonstrating the feasibility of the approach.

1. Introduction

The diffusion of decentralised small-scale renewable power generation sources is giving a boost to the development of smart nanogrids, particularly to increase the sustainability of electricity production and the efficiency of distribution. In order to ensure continuity of service, the reliability and maintainability of nanogrids are crucial problems that must be taken into account. Consequently, alongside management aspects connected with the generation and efficient use of renewable energy, there are also equally important aspects related with system maintenance and its automation via continuous monitoring. Monitoring and maintenance policies, in fact, can have a relevant impact on energy production, cost and waste, because they affect the quality and timing of restoring interventions and can significantly reduce downtime.

Thanks to its ubiquity and to the progress of photovoltaic (PV) technologies – which prompted significant cost reduction in the last decade – solar energy often plays a key role in micro- and nanogrids.

The power output of PV installations depends on several factors: environmental factors such as solar irradiance, temperature, dust deposition, and system factors such as module and inverter efficiencies; storage capabilities also play a significant role in the overall system performance by allowing some decoupling between energy production and demand.

In the first place, the energy output of a PV module is directly related to the incoming solar energy, irradiance varying according to weather conditions and the sun position. The module output current is approximately linearly dependent on the impinging irradiance level (G), hence the Maximum Power Point (MPP) is strongly related to irradiance. Consequently, module soiling due to dust accumulation etc., and the maintenance countermeasures aimed at assuring adequate conversion efficiency over the PV plant lifetime, must be factored in when making life-cycle economic estimates for PV installations.

Soiling is caused by dirt, dust and other particles covering the surface of the PV modules. The dust composition (pollutants, airborne liquid constituents, particulates, pollen), colour (due to different mineral composition) and the amount and type of soiling vary widely with plant location. The dust properties and its deposition rate are also affected by ambient conditions including humidity, wind speed and direction, and seasonal variations [1].

To counter the effects of soiling, panels must be periodically cleaned. This can be carried out with manual, mechanised, or robotic action by either wet or dry solutions, or by electrodynamic screen techniques.

At present, most PV arrays are inspected and cleaned with a scheduling that typically does not depend on the actual state of dirtiness and its effect on energy production efficiency. Neglecting the efficiency/maintenance trade-off may result in wasteful costs due to unnecessary cleaning actions. Therefore, an automated soiling sensing approach can be useful to develop a decision-making process accounting also for the trade-off between reliability of energy production, demand/offer matching, and cost. In this way, a supervisor can plan targeted interventions with optimal maintenance timing.

Detection of dust deposition, concentrated dirt or any soiling-related malfunction allows to decide when and what kind of cleaning is required, which calls for the development of a monitoring system with smart data management to automatically plan maintenance interventions, by combining weather forecasts and historical data, irradiance sensors and soiling sensors, and applying predictive algorithms. Refs. [2], [3], [4], [5] show studies of PV module cleaning protocols, while analysis of the effects of dirt and dust deposition can be found in [6], [7], [8], [9], [10].

A few soiling detection kits for medium/large scale plants have already been developed and marketed. A non-exhaustive list is reported in refs. [11], [12], [13], [14], [15], [16], [17]. These systems base their operation on the comparison of electrical measurements obtained from a clean reference module and from one exposed to soiling agents (except for the one in [14], which is based on LED and photodiode soiling ratio detection).

This work addresses the problem of PV module performance degradation due to soiling, with the aim of setting up a prototype sensor to detect dust deposition, thus helping distinguish between efficiency reduction due to dust and that due to degradation of PV modules or electronic components. The proposed system, based on a dust detection approach using both electrical sensing and optical inspection, is designed to be a low-cost solution for small-scale DC nanogrids operating either in grid-connected or islanded mode. In order to test the usefulness of the automated sensing approach, we developed a MATLAB/Simulink model of a smart nanogrid and estimated the economic benefits of the proposed approach and the optimum cleaning intervention rates.

2. Nanogrid Modeling

We developed a model of a DC nanogrid using the MATLAB/Simulink environment with the aim of testing different control strategies while assessing the usefulness of quantitative knowledge of PV modules soiling for maintenance policy

optimization. The Soiling Factor (SF) defined in [18] quantifies power losses due to dust accumulation by considering the percentage loss in equivalent irradiance reaching the module. The SF ratio is measured by the soiling sensor described in Section 3.

The model can simulate both islanded mode and grid-connected operation.

Fig. 1 shows the model's root level, where two independent nano-smart-grid (NSG) sub-models are instantiated. One (*NSG Dirty*) models the actual nanogrid operation, with a PV plant subjected to dust deposition effects; the other (*NSG Clean*) is a reference nanogrid model featuring perfectly clean PV modules. The *NSG* models run in parallel and are fed by the same scenario inputs, except for the soiling profile and the cleaning task activation trigger, which apply to *NSG Dirty* only.

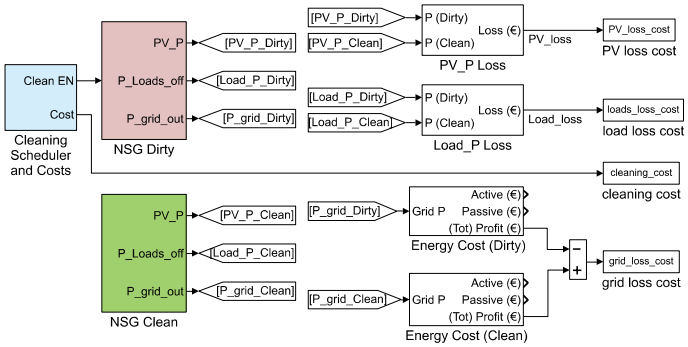

Fig. 1. Root level of the developed Simulink model.

The root level of the model (Fig. 1) also features energy cost computation blocks yielding quantitative information about economic losses due to soiling effects; economic losses are evaluated differently, depending on the nanogrid operation mode (islanded or grid-connected).

In the grid-connected scenario the focus is on the energy flow to and from the grid, and losses come from two main contributions: the reduction of energy exported to the grid, and the increase of energy import from the grid during shortfall phases. Starting from the power flowing out of the nanogrid (P_{grid}), we define exported (P_{out}) and imported (P_{in}) power flows (Eq. 1) which, integrated over time, yield the amounts of sold (E_{sold}) and purchased (E_{purch}) energy (Eq. 2). The prices per kWh of sold and purchased energy (R_{sold}, and R_{purch}, respectively) are then used to compute the revenue for energy sold (C_{sold}) and the expenditure for energy purchased (C_{purch}) (Eq. 3), and the overall energy cost (C_{tot}) for the nanogrid (Eq. 4).

$$P_{out} = \begin{cases} P_{grid}, & P_{grid} > 0 \\ 0, & P_{grid} \leq 0 \end{cases}, \quad P_{in} = \begin{cases} -P_{grid}, & P_{grid} < 0 \\ 0, & P_{grid} \geq 0 \end{cases} \tag{1}$$

$$E_{sold} = \int_0^{T_{stop}} P_{out}(t)\, dt\,, \quad E_{purch} = \int_0^{T_{stop}} P_{in}(t)\, dt \tag{2}$$

$$C_{sold} = R_{sold} \cdot E_{sold}, \quad C_{purch} = R_{purch} \cdot E_{purch} \tag{3}$$

$$C_{tot} = C_{sold} - C_{purch} \tag{4}$$

These equations are applied to both *Dirty* and *Clean NSG* models and, finally, the loss due to soiling is computed as:

$$C_{loss} = C_{tot}^{clean} - C_{tot}^{dirty} \tag{5}$$

When operating in islanded mode, losses come from the reduction of energy production due to soiling resulting in extra load shedding relative to the clean PV scenario. Thus, in this case, the power profiles of off-forced loads are integrated, the value of unsold energy is computed based on the price per kWh, and, finally, the economic loss relative to the clean-PV scenario is determined.

The cleaning task trigger and the total cost of cleaning interventions are generated and computed by the *Cleaning Scheduler and Costs* block, starting from cleaning frequency set-point input.

2.1 Nano-smart-grid (NSG) model

Our NSG model (Fig. 2) represents a typical office environment, powered by PV plant, featuring an energy storage system and a few DC loads, such as LED lamps, laptops, printers, tablets and smartphones. Fig. 2 in particular shows the *NSG Dirty* subsystem; *NSG Clean* differs from *NSG Dirty* in that the effects of dust deposition and cleaning interventions are neglected in the *Scenario* subsystem.

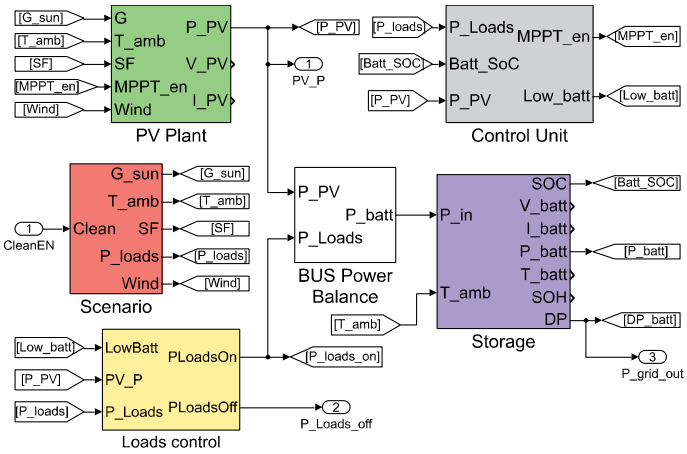

Fig. 2. View of the NSG Simulink sub-model (dirty case).

The *Scenario* block reads solar irradiance and load power profiles in workspace look-up-tables, as well as the values of ambient temperature and wind speed, and computes the SF as the integral over time of an average soiling rate that depends on the specific geographical location [19], [20]. SF saturates at 80%, and is reset at 0% every time a rising edge coming from *Cleaning Scheduler* is detected, signaling that a cleaning task has been carried out.

The *PV Plant* subsystem (Fig. 3) contains both the PV array model and the Maximum Power Point Tracking (MPPT) control algorithm. The PV module behaviour is described starting from 1-diode model equations [21], to which we added a static thermal model accounting for wind speed effect [22]. The 1-diode model parameters are computed starting from datasheet values. The MPPT controller can be enabled or disabled by the central control unit in order to achieve either MPPT or Load Power Tracking (LPT) operating modes. The latter is to be selected in islanded mode, when there is an excess of available energy, and storage is full. Under these conditions, the PV energy production is curtailed to satisfy load demand only. On the other hand, the MPPT controller observes the voltage setpoint and power output between the last 2 time-steps and determines the optimum current operating point on a virtual I-V characteristic [23]. The irradiance input (G) is reduced according to the SF, by computing a complementary cleanness factor (1-SF) (Fig. 3).

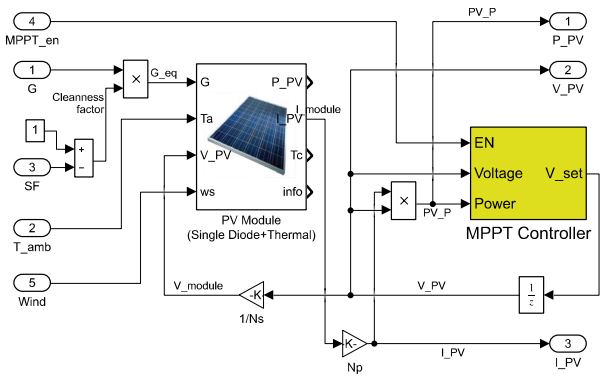

Fig. 3. PV plant subsystem comprising PV module model, MPPT controller, and the SF effect on the irradiance level.

The *Loads control block* implements a load shedding algorithm by assigning predefined priorities to loads. Knowing priority levels and load power profiles, according to the storage State of Charge (SoC) and PV power availability, loads are allowed to be on or disconnected.

The *Storage* subsystem models a lithium cell battery pack with its charging and control units based on a Constant Current/Constant Voltage (CC/CV) algorithm [24] and taking into account elementary thermal and aging behaviour. The DP signal injects the excess power from the PV block into the grid when the battery is fully charged, or absorbs the PV power deficit from the grid when the battery is discharged.

Finally, power balance is computed by the *BUS Power Balance* block, which calculates the energy flowing to the storage unit based on PV power production and load consumption.

The *Control Unit* subsystem coordinates energy flows by determining whether enabling or disabling the MPPT mode. In grid-connected mode MPPT is always enabled and all loads are connected.

2.2 Simulation results

Fig. 4 gives an example of results for the NSG subsystem obtained under a 2-days long scenario under three different soiling conditions: SF = 0 (clean modules), 10%, and 30%. Irradiance data from PVGIS [25] refers to Parma, Italy, Azimuth = 0°, Slope = 30°; typical load power profiles are from [26].

Some parametric simulations involving the whole model have been carried out in order to evaluate the economic loss due to dust deposition. Different scenarios have been considered so as to take into account various economic conditions and SF ratios. Results are given in Tab. 1, while an example of result is shown in Fig. 5 for the case of SF yearly increase rate of 0.06% (absolute), cost per cleaning intervention of 300 €, and energy price of 0.24 €/kWh and 0.18 €/kWh for buying and selling, respectively. In all scenarios the final cost is evaluated just before the plant end-of-life (30 years). Tab. 1 shows that cleaning interventions are much more convenient in grid-connected nanogrids. In islanded mode, on the other hand, often PV and storage systems are oversized in order to minimize the occurrence of load shedding. Therefore, the PV plant often operates in LPT mode, and performance loss due to soiling has no significant impact. It should be noted that in this paper the energy deficit (causing load shedding) was given the same economic value as that of energy purchased from the grid; this assumption has no universal value, and should therefore be modified depending on the specific operational context.

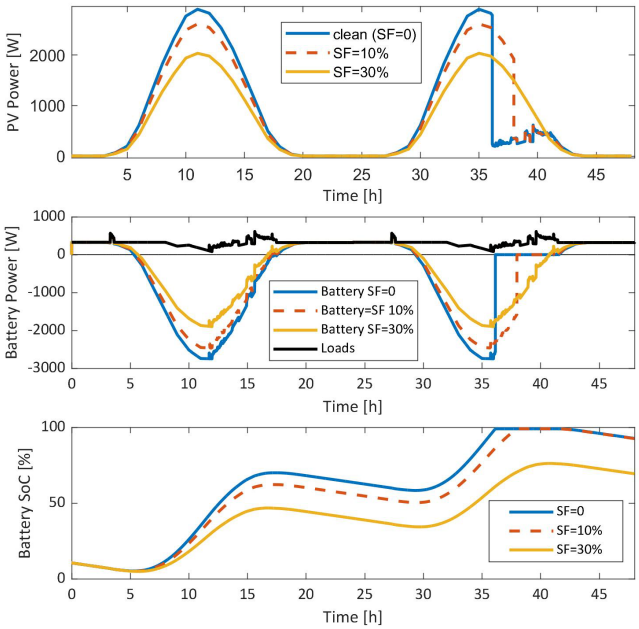

Fig. 4. Simulation results obtained with 0 (clean PV array), 10%, and 30% SF. Irradiance profile from June 21-22 scenario in Parma (Italy). PV array maximum power rate = 3 kWp, Azimuth = 0°, Slope = 30°.

Cleaning cost [€/intervention]	Energy price [€/kWh]		SF rate [%/year]	Optimal scheduling interval [years]	
	Buying	Selling		Grid connected	Islanded
150	0.18	0.13	0.015	3	10
150	0.18	0.13	0.03	2	6
150	0.18	0.13	0.06	1.5	3.75
150	0.18	0.13	0.09	1	15.75
150	0.18	0.13	0.12	1	15.75
150	0.24	0.18	0.015	2.5	10
150	0.24	0.18	0.03	1.75	6
150	0.24	0.18	0.06	1.25	3.75
150	0.24	0.18	0.09	1	15.75
150	0.24	0.18	0.12	1	15.75
200	0.18	0.13	0.015	3	15.75
200	0.18	0.13	0.03	2.5	7.5
200	0.18	0.13	0.06	1.5	15.75
200	0.18	0.13	0.09	1.25	15.75
200	0.18	0.13	0.12	1	15.75
200	0.24	0.18	0.015	3	10
200	0.24	0.18	0.03	2	6
200	0.24	0.18	0.06	1.5	3.75
200	0.24	0.18	0.09	1	15.75
200	0.24	0.18	0.12	1	15.75
290	0.18	0.13	0.015	3.75	15.75
290	0.18	0.13	0.03	3	7.5
290	0.18	0.13	0.06	2	15.75
290	0.18	0.13	0.09	1.5	15.75
290	0.18	0.13	0.12	1.5	15.75
290	0.24	0.18	0.015	3	15.75
290	0.24	0.18	0.03	2.5	7.5
290	0.24	0.18	0.06	1.5	15.75
290	0.24	0.18	0.09	1.5	15.75
290	0.24	0.18	0.12	1	15.75

Tab. 1. Comprehensive report of the results obtained with multi scenario simulations.

3. Soiling Sensor

The main goal of this work is the development of a soiling sensing approach that applies two techniques in parallel, namely, I-V curve analysis [27] and optical inspection [28], to quantify the degradation and qualify the dirt accumulated on PV modules, respectively.

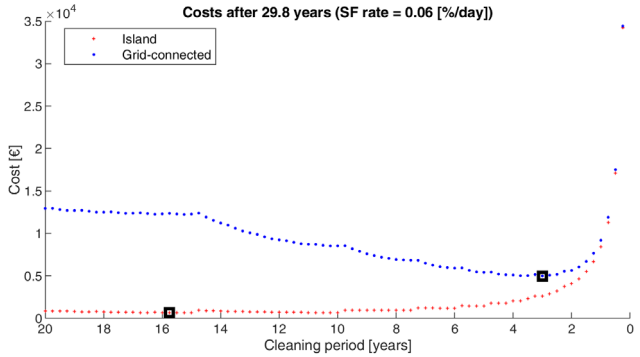

Fig. 5. A simulation scenario: case of 0.06%/year SF ratio, cleaning intervention cost of 300 €, energy cost of 0.24 €/kWh and 0.18 €/kWh for selling and buying respectively.

The sensor consists of a small off-grid PV module employed as a reference for dust analysis. Detailed information about the two different modules employed in the experiments can be found in Tab. 2. We developed an acquisition board for module electrical performance characterization, and used a camera to take photos of the module to be processed by MATLAB optical analysis algorithms.

S. E. Project SEM25M (c-Si)	
Open circuit voltage (V_{oc})	21.3 V
Short circuit current (I_{sc})	1.6 A
Maximum Power rating (P_{max})	25 W
Active area (A)	1869 cm^2

ICO-SPT-40W (thin-film)	
Open circuit voltage (V_{oc})	24 V
Short circuit current (I_{sc})	2.88 A
Maximum Power rating (P_{max})	40 W
Active area (A)	4293 cm^2

Tab. 2. Reference modules factory data.

3.1. I-V curve analysis

In order to measure the I-V curve of the PV reference module we built an acquisition board (Fig. 6) equipped with a power MOSFET acting as an active load.

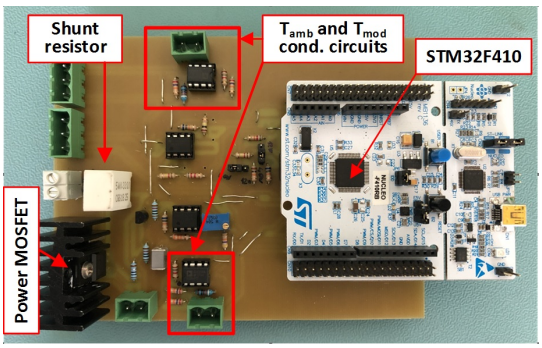

Fig. 6. I-V slope acquisition board.

An STM32 microcontroller generates a PWM wave, which is input to a low-pass filter. The duty-cycle is varied to obtain a DC voltage sweep that is applied to the transistor gate, thereby varying its channel resistance, from below threshold to fully-on state, hence obtaining a sweep from open circuit to short circuit for the PV module load.

Under each load condition, the current and voltage across the module are sampled by the microcontroller ADC, after being properly conditioned by onboard signal attenuation circuits. The voltage drop across a shunt resistor is used to measure the magnitude of the current. The acquisition board is also equipped with circuits suitable for measuring the ambient temperature and the cell temperature by means of PT1000 thermistors. The collected data are finally sent to a computer where a MATLAB script performs the necessary processing tasks. The electrical and logical structure of the board is shown in Fig. 7.

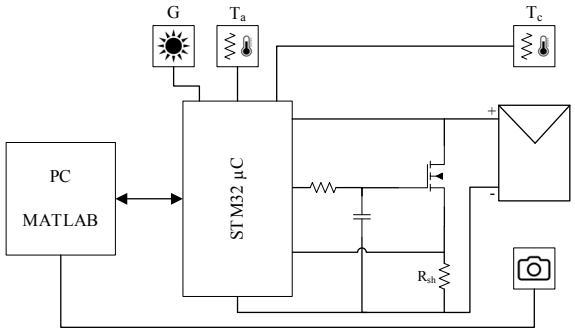

Fig. 7. Schematic diagram of the soiling sensing system.

3.2. Optical inspection

The optical analysis is performed by taking digital photos of the module from a fixed position. A MATLAB script processes the image by artificial vision algorithms to calculate the amount of the soiled area. The process starts with a photo of the clean module, which serves the purpose of the masking step that is necessary to cut out non-active areas, such as the frame and cell interconnect metallization. Four red markers serve as reference points for the geometric transformation that removes deformation effects due to perspective.

Fig. 8 shows the flowchart of the overall image analysis process. First the image object is loaded and the position of the markers detected. Second, the image is binarized applying appropriate color threshold levels. Third, the image is cropped and de-warped with the help of the markers. The image is then resized, if its size differs from the reference image. Finally, pixel analysis is performed, and the dust-covered area is determined. In addition, the algorithm detects sub-areas characterized by different kind of depositions, thus allowing to establish if the dust distribution is uniform or aggregated in spots. Quantitative data is output on the percentage of covered area, the area of the widest spot (if any), and the prevailing color component (useful in determining the type of dirt).

4. Results and discussion

Experiments were performed artificially depositing a weighted amount of dust on the reference module. Dust is collected from area surrounding the module. It is obtained by finely sieving some dry soil, resulting in a mixture of potting soil, sand, etc. This technique allows only particles with a diameter < 0.5 mm to pass through. Then, dust is spread on the reference module, which was preventively cleaned. The selected amount of powder is quantified by means of a precision scale with 1 mg accuracy. To avoid powder to be dispersed, a thin layer of water is sprayed on the module. This also allows to emulate the effects of rain and dew effects on dust deposition. Once the module has dried the analysis procedure starts: the I-V curve is acquired in parallel with irradiance, ambient temperature and

cell temperature (a PT1000 sensor is tightly attached behind the PV reference module in correspondence with a cell). Meanwhile, a photo of the module is taken and processed.

In Fig. 9 we show some results obtained with I-V characteristics extraction for different amount of dust, for a c-Si (Fig. 9a) and for a thin-film module (Fig. 9b). Tests are performed for each module at constant irradiance and ambient temperature.

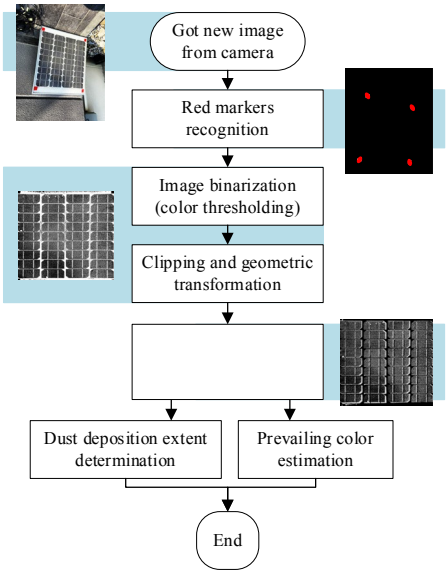

Fig. 8. Optical inspection algorithm flowchart.

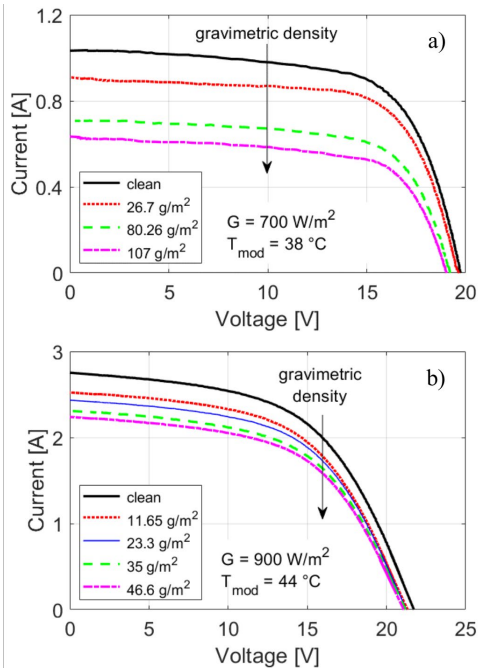

Fig. 9. I-V characteristics obtained for different soiling levels: a) c-Si module, while b) thin-film module.

From each curve, the MPP is determined. MPPs are plotted in Fig. 10, normalized with respect to the STC value, showing a quite linear relationship between the amount of deposited dust and power loss. The extracted slopes are about $1.7 \cdot 10^{-3}$ $(g/m^2)^{-1}$ and $1.9 \cdot 10^{-3}$ $(g/m^2)^{-1}$ for c-Si and thin-film, respectively.

Optical analysis has also been performed on the reference modules. Results for two different dust distributions are shown in Fig. 11. Case a) shows a uniform powder distribution on a c-Si module, resulting in a detected covered area of 36%; in case b) dust is deposited on a thin-film panel in non-uniform random stains, resulting in 10% coverage.

Finally, Fig. 12 illustrates an early result obtained applying a new soiling technique in which dust is deposited using compressed air. This allows to obtain uniformity levels similar to the ones reached with aerosol method [27] but much more quickly. In future experiments we will combine morphological and chemical analysis with this deposition technique with the aim of obtaining accurate qualitative and quantitative relationships between the amount of deposited dust and the MPP reduction.

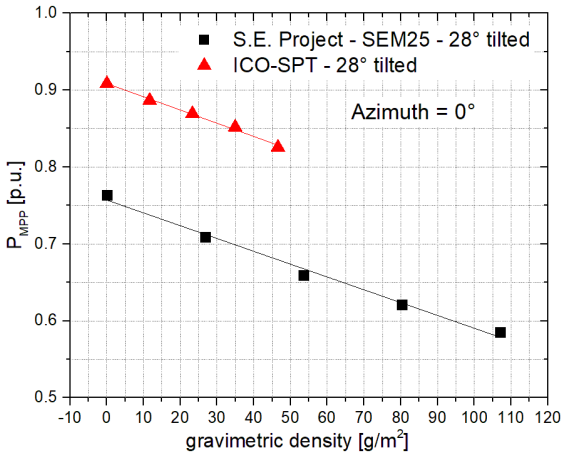

Fig. 10. Computed relationship between deposited dust density and normalized MPP.

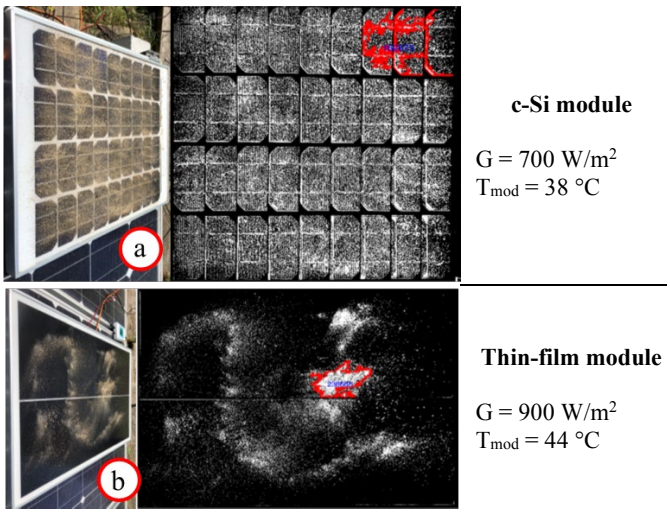

Fig. 11. Optical analysis results. a) Uniform dust deposition on c-Si module (36% covered area); b) stain-like deposition on thin-film module (10% covered area). The camera viewport is parallel to the ground while modules are tilted by about 28°.

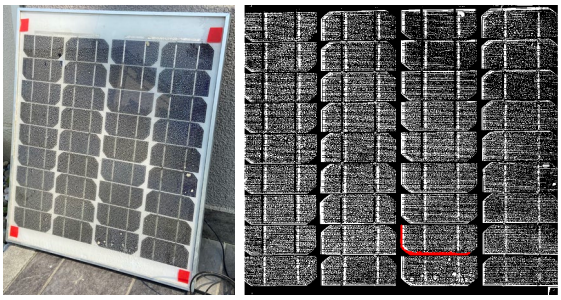

Fig. 12. Photo of the c-Si PV module with compressed-air deposited dust (left) and image after MATLAB elaboration (right). Estimated heavily covered area: about 30%.

5. Conclusions

This work addresses the problem of PV module performance degradation due to soiling, by developing a prototype sensing system for dust deposition, with the goal of distinguishing the efficiency reduction due to dust from other degradation modes, and deploying cleaning interventions accordingly.

In order to assess the usefulness of the automated sensing approach, and the optimization of cleaning protocols it allows, we have built a MATLAB/Simulink model of a smart-nano-grid and estimated the economic benefits of the proposed approach and the optimum cleaning intervention rates for various scenarios differing by energy price, soiling rate, and operating mode (grid-connected or islanded).

Early experiments show the feasibility of the proposed sensing approach, which is based on a combination of electrical analysis and automated optical inspection.

This solution can be used for automated smart maintenance of PV plants to reduce downtime and keep efficiency at its maximum, considering the trade-off between maintenance cost and losses due to soiling.

References

[1] T. Sarver, A. Al-Qaraghuli, and L. Kazmerski, A comprehensive review of the impact of dust on the use of solar energy: History, investigations, results, literature, and mitigation approaches, Renewable and Sustainable Energy Reviews 22 (2013), pp. 698-733.

[2] D. L. Alvarez, A. S. Al-Sumaiti, and S. R. Rivera, Estimation of an Optimal PV Panel Cleaning Strategy Based on Both Annual Radiation Profile and Module Degradation, IEEE Access vol. 8 (2020), pp. 63832-63839.

[3] H. Mei, Z. Shen and C. Zeng, Study on cleaning frequency of grid-connected PV modules based on Related Data Model, 2016 IEEE International Conference on Power and Renewable Energy (ICPRE), Shanghai, 2016, pp. 621-624.

[4] M. Naeem and G. Tamizh Mani, Cleaning frequency optimization for soiled photovoltaic modules, 2015 IEEE 42nd Photovoltaic Specialist Conference (PVSC), New Orleans, LA, 2015, pp. 1-5.

[5] Z. Wang, Z. Xu, Y. Zhang and M. Xie, Optimal Cleaning Scheduling for Photovoltaic Systems in the Field Based on Electricity Generation and Dust Deposition Forecasting, IEEE Journal of Photovoltaics, (2020), pp. 1-7.

[6] S. Warade and A. Kottantharayil, Analysis of Soiling Losses for Different Cleaning Cycles, 2018 IEEE 7th World Conference on Photovoltaic Energy Conversion (WCPEC) (A Joint Conference of 45th IEEE PVSC, 28th PVSEC & 34th EU PVSEC), Waikoloa Village, HI (2018), pp. 3644-3647.

[7] A. Gholami, M. Ameri, M. Zandi, R. G. Ghoachani, S. Eslami and S. Pierfederici, Photovoltaic Potential Assessment and Dust Impacts on Photovoltaic Systems in Iran: Review Paper, in IEEE Journal of Photovoltaics, vol. 10, no. 3 (2020), pp. 824-837.

[8] Z. Abderrezzaq, M. Mohammed, N. Ammar, S. Nordine, D. Rachid and B. Ahmed, Impact of dust accumulation on PV panel performance in the Saharan region, 2017 18th International Conference on Sciences and Techniques of Automatic Control and Computer Engineering (STA), Monastir (2017), pp. 471-475.

[9] H. A. Badi, J. Boland, D. Bruce and M. Albadi, Dust Event Impact on Photovoltaic Systems: Role of humidity in soiling and self-cleaning, 2018 IEEE International Conference on Smart Energy Grid Engineering (SEGE), Oshawa, ON (2018), pp. 342-345.

[10] Z. Wu, W. Li, S. Kuka and M. Alkahtani, Analysis of Dust Deposition on PV Arrays by CFD Simulation, IECON 2019 - 45th Annual Conference of the IEEE Industrial Electronics Society, Lisbon, Portugal (2019), pp. 5439-5443.

[11] Ammonit. Soiling Measurement for PV Power Plants. [online] Available at: https://www.ammonit.com/en/component/content/article/165-ammonit-messsysteme/solar-resource-assessment/407-solar-resource-assessment [Accessed 2 April 2020].

[12] NRG Systems. Soiling Measurement for PV Power Plants. [online] Available at: https://www.nrgsystems.com/products/solar/detail/soiling-measurement-kit0 [Accessed 2 April 2020].

[13] Campbell Scientific. Solar-Module Performance Monitoring System. [online] Available at: https://www.campbellsci.com/smp100 [Accessed 2 April 2020]

[14] Kipp&Zonen. DustIQ for Soiling Monitoring of PV. [online] Available at: https://get.otthydrometinsights1.com/kippzonen/dustiq/ [Accessed 2 April 2020]

[15] Atonometrics. PV Device Soiling Measurement Systems for PV Power Plants. [online] Available at: http://www.atonometrics.com/products/soiling-measurement-system-for-pv-modules/ [Accessed 2 April 2020]

[16] Kintech Engineering. Soiling measurement kit. [online] Available at: https://www.kintech-engineering.com/products/soiling-measurement-kit/soiling-measurement-kit/ [Accessed 2 April 2020]

[17] Moroni & Partners. PV Cleaning Optimizer. [online] Available at: http://www.pvcleaning.com/ [Accessed 2 April 2020]

[18] P. Cova, N. Delmonte, M. Lazzaroni, Photovoltaic plant maintainability optimization and degradation detection: Modelling and characterization, Microelectronics Reliability, Volumes 88–90 (2018), pp. 1077-1082.

[19] D. Dahlioui, B. Laarabi, M. A. Sebbar, A. Barhdadi, G. Dambrine, E. Menard, J. Boardman, Soiling effect on photovoltaic modules performance: New experimental results, 2016 International Renewable and Sustainable Energy Conference (IRSEC), Marrakech (2016), pp. 111-114.

[20] M. R. Maghami, H. Hizam, C. Gomes, M. A. Radzi, M. I. Rezadad, S. Hajighorbani, Power loss due to soiling on solar panel: A review, Renewable and Sustainable Energy Reviews, Volume 59 (2016), pp. 1307-1316.

[21] S. Vergura, A Complete and Simplified Datasheet-Based Model of PV Cells in Variable Environmental Conditions for Circuit Simulation, Energies 9 (2016), 326.

[22] C. Schwingshackl, M. Petitta, J.E. Wagner, G. Belluardo, D. Moser, M. Castelli, M. Zebisch, A. Tetzlaff, Wind Effect on PV Module Temperature: Analysis of Different Techniques for an Accurate Estimation, Energy Procedia 40 (2013), pp. 77-86.

[23] T. Jayakumaran, G. Gurunathau, C. V. Srlkanth, M. K. Shashank, R. Venkatesh, B. Ramkiran, P. Neelamegam, A Comprehensive Review on Maximum Power Point Tracking Algorithms for Photovoltaic Cells, 2018 International Conference on Computation of Power, Energy, Information and Communication (ICCPEIC), Chennai (2018), pp. 343-349.

[24] W. Shen, T. T. Vo, and A. Kapoor, Charging algorithms of lithium-ion batteries: An overview, 2012 7th IEEE Conference on Industrial Electronics and Applications (ICIEA), Singapore (2012), pp. 1567-1572.

[25] T. Huld, R. Müller, and A. Gambardella, 2012: A new solar radiation database for estimating PV performance in Europe and Africa, Solar Energy 86, pp. 1803-1815. https://re.jrc.ec.europa.eu/pvg_tools/it/tools.html

[26] A. Reinhardt, P. Baumann, D. Burgstahler, M. Hollick, H. Chonov, M. Werner, R. Steinmetz, On the accuracy of appliance identification based on distributed load metering data, 2012 Sustainable Internet and ICT for Sustainability (SustainIT), Pisa (2012), pp. 1-9.

[27] J. J. John, S. Warade, G. Tamizhmani and A. Kottantharayil, Study of Soiling Loss on Photovoltaic Modules With Artificially Deposited Dust of Different Gravimetric Densities and Compositions Collected From Different Locations in India, IEEE Journal of Photovoltaics, vol. 6, no. 1 (2016), pp. 236-243.

[28] T. Pivem, F. Araújo, L. D. Araujo, G. S. Oliveira, Application of A Computer Vision Method for Soiling Recognition in Photovoltaic Modules for Autonomous Cleaning Robots, Signal & Image Processing: An International Journal, 10 (2019), pp. 43-59.